Supporting Information for the Manuscript:
FCS diffusion laws on two-phases lipid membranes : experimental and Monte-carlo simulation determination of domain size.

Cyril Favard, Jérôme Wenger,
Pierre-François Lenne, Hervé Rigneault

January 4, 2011

Content of the supporting information

In the supporting information are given :

- Material and methods, describing in detail the lipids and the dye used for the experiments, the preparation of multilamellar vesicles, the FCS setup, the model used to fit the autocorrelation functions, the algorithm used for Monte Carlo simulation of the lipid thermodynamics and the obtention of FCS diffusion laws resulting from this simulation and finally the analysis by means of ICS and morphometry of the images generated by MC simulation.

- A figure (Fig. 1) that plot the values of effective diffusion coefficient as a function of temperature found in the FCS diffusion laws. These values can be compared to the one found by Vaz *et al.* (1).

- A heuristic model explaining the negative diffusion time at zero waist by using analogy to the mesh case in (2) and a figure (Fig. 2) showing accuracy of the predicted diffusion time at zero waist by this model and the one numerically and experimentally found. A movie (Movie S1) supporting this heuristic model by showing that the diffusion is restricted by the presence of solid domains and size fluctuation of these domains.

- A justification of the choice of Bodipy C5 PC as the dye used for determination of experimental domain mean size on lipids and a figure (Fig. 3) comparing the mean size of the domains seen by experimental FCS diffusion laws on DMPC:DSPC 8:2 mol:mol mixture using a fluorescent head labeled phospholipid (Atto647 PE) or a fluorescent chain labeled phospholipid (Bodipy C5 PC).
- An explanation of the fit of the FCS diffusion laws using anomalous diffusion model in the case of the DMPC:DSPC 8:2 mol:mol mixture, and a related figure (Fig. 4) exhibiting two minima for the anomalous exponent for temperatures close to the two transition temperatures : $gg : gf$, $gf : ff$.
- A table containing all the symbols and their signification (Table 2) used in the supporting information

1 Material and Methods

1.1 Material

The lipids 1,2-distearoyl-*sn*-glycero-3phosphocoline (DSPC) and 1,2-dipalmitoyl-*sn*-glycero-3-phosphocholine (DMPC) were purchased from Avanti Polar Lipids (Alabaster, AL.). They were used without further purification and kept at $-20\,^{\circ}$C in chloroform:methanol(9:1, mol:mol) at 100mM concentration. For FCS measurements lipids mixtures were labeled with 2-(4,4-difluoro-5,7-dimethyl-4-bora-3a,4a-diaza-s-indacene-3-pentanoyl)- 1-hexadecanoyl-*sn*-glycero-3-phosphocholine(β-BODIPY FL C5-HPC)from Invitrogen (Carlsbad, CA, USA)).

1.2 Preparation of multilamellar vesicles

10 μl of a 10mM mixture of DMPC:DSPC (8:2 mol:mol), labeled with β Bodipy Fl C5-HPC at a lipid molar ratio of 1:50 000, were deposited on a glass coverslip previously extensively cleaned with ethanol, water:ethanol (7:3 vol:vol) and chloroform. Lipids were dried under vacuum for one hour and hydrated with 700 μl of pure distilled water previously heated at $50\,^{\circ}$C. Sample was then allowed to cool down for at least 30 min to the different measurement temperatures within the microscope chamber.

1.3 FCS experiments

FCS experiments were performed on a home-built device. This experimental setup has been extensively described in (3). Briefly, it is based on an inverted microscope (Zeiss Axiovert 35M) with a NA=1.2 water immersion objective (Zeiss C-Apochromat) and a three-axis piezo-scanner (Physik Instrument, Germany). In order to avoid photobleaching of the fluorescent label during the experiment 3μW of a CW laser at 488nm was used for fluorescence excitation. A 30μm pinhole conjugated to the microscope object plane, defines the observation volume. After the pinhole, the fluorescence signal is split by a 50/50 beamsplitter and focused on two avalanche photodiodes (Perkin-Elmer SPCM-AQR-13) through a 535 ± 20 nm fluorescence bandpass filters (Omega Filters 535DF40). The fluorescence intensity fluctuations are analyzed by cross-correlating the signal of each photodiode with a ALV6000 hardware correlator. For FCS diffusion laws, waist of the laser in the object plane was modified by underfilling the microscope objective back-aperture using an adjustable diaphragm placed on the excitation optical path. The values of the observation area therefore obtained were calibrated by measuring the diffusion time of a 0.5 μM Rhodamine-6G in aqueous solution at 22 $^\circ$ C (D=280 $\mu m^2.s^{-1}$). For each waist at each temperature of the study, at least 200 FCS measurements of 10s duration each were made by series of 10. Experiments were made in a chamber designed around the entire microscope in order to avoid any temperature gradient between the sample and the microscope objective. The temperature was set to the chosen value by means of a commercial temperature controller (The Cube, Life Imaging Services, Switzerland). Accuracy was measured to be within $\pm 0.1 K$at the sample position by means of home built digital thermometer.

1.4 Fitting of ACFs

For free Brownian two-dimensional diffusion in the case of a Gaussian molecular detection efficiency and accounting for negligible photophysics effects on the fluorophore (triplet state, blinking, bleaching...) the fluorescence autocorrelation function (ACF) is given by :

$$g^{(2)}(\tau) = 1 + \frac{1}{N} \frac{1}{1 + \frac{\tau}{\tau_d}} \tag{1}$$

where N denotes the average number of molecules in the observation area and τ_d the diffusion time. τ_d is linked to the laser beam transversal waist w

and the molecular diffusion coefficient D by :

$$\tau_d = \frac{w^2}{4D} \tag{2}$$

All the ACFs obtained experimentally or in Monte-Carlo simulations were fitted using Eq. 1.

1.5 Monte Carlo simulation of the two phases two components lipid mixture

Our Monte Carlo simulations were directly adapted from the work of Sugar *et al.* (4) also described in (5). Briefly, the thermal fluctuations of the DMPC : DSPC lipid mixture was simulated using a two-state Ising type monolayer triangular lattice. Each lattice point is occupied by one acyl chain of either DMPC or DSPC. During the simulation,trial configuration are generated by means of six different elementary steps :
- One that can be described as a **phase transition step**, consists in changing the state of a randomly selected acyl chain from gel to fluid or inversely.
- Five that can be described as **diffusion steps**, consist in exchanging two neighboring molecules.
In the Monte Carlo algorithm, 3 different processes can occur at 3 different time scales. One is diffusing in a liquid environment, the other is diffusing in gel environment and the last is changing its state. For lipids within a mixed environment (both gel and fluid), the probability of entering a diffusion step depends on the fraction of lipids chains in gel state ($f_{c,g}$) surrounding the two lipids that are to enter a diffusion step. As extensively described in (5), a rate function $r(f_{c,g})$ has been introduced in the simulation :

$$r(f_{c,g}) = r_0 exp(-f_{c,g}\frac{\Delta E}{kT}) \tag{3}$$

where r_0 is the value of $r(f_{c,g})$ in a fully liquid environment ($f_{c,g} = 0$) and ΔE is the energy barrier needed for a diffusion step in an all-gel environment ($f_{c,g} = 1$). As in the work of Hac *et al.* (5), the phase transition step probability (r_{state}) was set to be equal to r_0 and $\Delta E/kT$ was set to 4.25 according to the following ratio : $\frac{D_f}{D_g} = 70$

1.6 Thermodynamic model

The thermodynamic model used here is extensively described in (4) and (5). Briefly, each lipid chain can exist in two states, gel(g) of fluid(f), these

states being different in internal energy as well as in entropy. Therefore the total energy of one layer of the lipids in a given configuration C is given by :

$$\begin{aligned} E(C) = n_A^g E_A^g + n_A^f E_A^f + n_B^g E_B^g + n_B^f E_B^f \\ + n_{AA}^{gg} E_{AA}^{gg} + n_{AA}^{gf} E_{AA}^{gf} + n_{AA}^{ff} E_{AA}^{ff} + n_{AB}^{gg} E_{AB}^{gg} \\ + n_{AB}^{gf} E_{AB}^{gf} + n_{AB}^{fg} E_{AB}^{fg} + n_{AB}^{ff} E_{AB}^{ff} + n_{BB}^{gg} E_{BB}^{gg} + n_{BB}^{gf} E_{BB}^{gf} + n_{BB}^{ff} E_{BB}^{ff} \end{aligned} \quad (4)$$

where $n_{A,B}^g$ and $n_{A,B}^f$ are the numbers of the gel and fluid lipid chains and the $E_{A,B}^g$ and $E_{A,B}^f$ terms are the respective internal energies of the two states of species A and B. It is shown in (4) that the Gibbs free energy for a given state can be written as :

$$\begin{aligned} G = G_0 + n_A^f(\Delta H_A - T\Delta S_A) + n_B^f(\Delta H_B - T\Delta S_B) \\ + n_{AA}^{gf}\omega_{AA}^{gf} + n_{BB}^{gf}\omega_{BB}^{gf} + n_{AB}^{gg}\omega_{AB}^{gg} + n_{AB}^{ff}\omega_{AB}^{ff} + n_{AB}^{gf}\omega_{AB}^{gf} + n_{AB}^{fg}\omega_{AB}^{fg} \end{aligned} \quad (5)$$

Where ΔH_A and ΔH_B are the calorimetric enthalpies, $\Delta S_A = \frac{\Delta H_A}{T_{m,A}}$ and $\Delta S_B = \frac{\Delta H_B}{T_{m,B}}$ are the respective melting entropies with $T_{m,A}$ and $T_{m,B}$ being the melting temperatures of the two pure components and G_0 the energy of an all gel lipid matrix. All the other parameters ($\omega_{ij}^{\alpha\beta}$) are the nearest-neighbor interaction parameters of a lipid chain species i in state α with a lipid chain species j in state β. The whole set of parameters described above has been given values according to (5) since these values have been obtained on multilamellar vesicles. These values are summarized in table 1.

1.7 FCS diffusion laws in the Monte Carlo simulations

In order to build FCS diffusion laws in the MC simulations, 20% of the total number of DMPC lipids chains were introduced as markers. During the simulation, these lipids move and generate intensity according to their position in the laser profile which is considered as a Gaussian with a given waist w(value of the radius at $1/e^2$ intensity),

$$I(r) \propto exp(-\frac{2(r-r_0)^2}{w^2}) \quad (6)$$

At each time step, the detected intensity in our simulations is computed assuming a Poisson distribution. The number of detected photons (n_{ph}) for a particle at position (x,y) is given by a random variable following the Poisson distribution with parameter βI(x,y) with β describing the collection efficiency of the setup (6).

To analyse intensity fluctuations, the normalized time autocorrelation function (ACF) is defined as :

$$g^{(2)}(\tau) = \frac{< n_{ph}(t) n_{ph}(t+\tau) >}{< n_{ph}(t) >^2} \tag{7}$$

where $< . >$ represents a time average. In our simulations, the ACF is calculated from a generated intensity file after the whole Monte Carlo simulation. The software correlator used to compute the ACFs follows the architecture proposed by (7) and described in (6). It has a logarithmic timescale, each channel having an individual sampling time and delay time.

FCS diffusion laws are then built by correlating the intensity fluctuations obtained at different waist in the same simulation. The biggest waist being $2/3^{rd}$ of the simulated matrix.

1.8 Image analysis

While running Monte-Carlo simulations, some images of the lattice were recorded at a chosen Monte Carlo step frequency, using an intensity code for the four different combination of the lipids states (I_{gf}^{AB}). This lead to an easier numerical image analyze capacities for thresholding.

Image correlation spectroscopy (ICS) analyzes were conducted on thresholded binary images using the ICS plugin for ImageJ ($http://rsb.info.nih.gov/ij/$) developed by Fitz Elliott, based on the work of Petersen (8) which can be found at $http://www.cellmigration.org/resource/imaging/software$. A 2D correlogram of our images obtained from the MC simulation was generated using the spatial image correlation spectroscopy module of the plugin. This 2D correlogram was reduced to a monodimensional correlogram assuming a circular symmetry. The 1D correlogram was arbitrary fitted by the following biexponential function :

$$g(\xi) = g(0)(a_1.e^{-(\xi/l_{c1})} + a_2.e^{-(\xi/l_{c2})}) + g(\infty) \tag{8}$$

where $l_{c_1} < l_{c_2}$, each parameter's significance is discussed in the results section. Correlograms were averaged over 50 different images of the MC simulation at each temperature. The performance of this procedure was tested using simulated images of circular domains of different radius and showed error within 20 % accuracy.

Direct morphoanalysis was performed using the ImageJ plugin "particle analysis". Analysis are conducted on binary thresholded image over the same set of 50 different images as the one used for ICS. The "particle anaylsis" plugin is a simple binary derivative method that delimits areas of pixels

having the same value (1 or 0) therefore giving a direct access to the number and area of the domains on each image. This method allows to plot the exact distribution in term of area and occurrence of the domains. For simplicity reason, it was decided to keep only the mean area of the domains defined as the following :

$$A_{dom} = \frac{1}{N} \sum_{A=2}^{A=\infty} N_A A \tag{9}$$

with A the value of the area (split in different classes every 25 pixels) and N the number of occurrence of this area within the image.

Finally, the fractional area of gel lipids (S_g^n) defined as the following $S_g^n = \frac{S_g}{S_g + S_f}$ within the image could also be determined at each temperature using this method, allowing therefore to scale the image in nm. This fraction was used to extrapolate the total area of the simulation and the mean area ($\langle a \rangle = f_g.a_g + f_f.a_f$) occupied by a lipid according the following value of lipid areas, $a_f = 63\mathring{A}^2$ and $a_g = 45\mathring{A}^2$ for PC lipids (9, 10).

2 Effective diffusion coefficient found in the FCS diffusion laws

Effective diffusion coefficient can be extracted from the FCS diffusion laws by measuring the slope of the asymptotically linear extrapolated laws (see main text for detailed explanations). They are plotted in Fig. 1 for both DMPC and DMPC:DSPC 8:2 mol:mol mixtures using experimental or numerical approach. The experimentally obtained results for this D_{eff} show a very high similarity to the one already found by Vaz *et al.*, (1) by FRAP experiments in DMPC:DSPC 80:20 mol:mol mixtures.

3 Origin of negative diffusion time at zero waist

As shown in Fig 2C and 2D or Fig 5C and 5D of the main text, τ_{d_0} extrapolated from the fit of the FCS diffusion laws (both experimental and simulated) using Eq.5 of the main text, exhibit growing negative value with decreasing temperature.

The results obtained here are close to the one obtained by Wawrezinieck *et al.* (2) for a mesh of partially permeable barriers. In this later case, it is shown that the FCS diffusion law can be correctly described by the following equations :

$$\tau_d = \begin{cases} \frac{w^2}{4D_{micro}} & \text{if } X_c^2 < 2 \\ S_{conf}\frac{w^2}{4D_{micro}} + k(\tau_d^{domain} - \tau_{conf}) & \text{if } X_c^2 > 2 \end{cases} \quad (10)$$

Where D_{micro} is the local diffusion coefficient, τ_d^{domain} is the characteristic diffusion time inside a mesh, τ_{conf} is the confinement time defined as $S_{conf}\tau_d^{domain}$ and S_{conf} is the strength confinement that is a function of the probability to cross a barrier to go from one mesh to another, giving therefore an indication on the stiffness of the barrier. X_c^2 being the normalization of the waist (w) to the meshsize *(a)* and defined in the case of a square meshwork as $X_c^2 = \frac{\pi w^2}{4a^2}$. It has to be noted that for $X_c^2 > 2$ Eq 10 can be rewritten as :

$$\tau_d = S_{conf}\frac{w^2}{4D_{micro}} + k\tau_d^{domain}(1 - S_{conf}) \quad (11)$$

In the case of the DMPC:DSPC mixture, one can simplify the system to a two state (gel and fluid) system with for each a typical diffusion time τ_d^g and τ_d^f exist. In the case of the MC simulation, at a given waist, it has been chosen that $\tau_d^g = 70\tau_d^f$. Since τ_d^g is much more than τ_d^f, when a tracer moves into a gel environment it can appear as being strongly confined to this environment as compared to the same tracer into a fluid environment. Therefore, gel domains can be considered as barriers to free diffusion of the molecule in the liquid phase. It can be clearly seen from a movie issued from MC simulation (see the movie online) that the tracer molecules move freely in the fluid environment while they seem to be unable to cross a gel environment at least during the duration of the movie (300 MC steps). The movie also show that their probability of escaping the solid domains are linked to the fluctuations in the size of the domain itself. Therefore, by analogy to the mesh of partially permeable barriers case described here above, τ_{conf} could be defined as a function of τ_d^g times the normalized surface of gel (S_g^n) that has to be crossed by the tracer molecule.

FCS diffusion law obtained in this study could be described by the following simple intuitive model :

$$\tau_d = \begin{cases} \frac{w^2}{4D_{micro}(T)} & \textbf{\textit{if}}\ w^2 < Bw_0^2 \\ S_g^n\frac{w^2}{4D_{micro}(T)} + K(\tau_d^f - S_g^n\tau_d^g) & \textbf{\textit{if}}\ w^2 > Bw_0^2 \end{cases} \quad (12)$$

With K and B given dimensionless constants and w_0^2 the value of w^2 for $\tau_d = 0$.

Eq 12 shows that the first part of the FCS diffusion law, below the cross over regime, is linked to the local diffusion constant D_{micro} which is a function of the temperature. In the MC simulation, D_{micro} has been defined such that $D^f_{micro} = 70D^g_{micro}$. By linear fit of the simulated FCS laws at small waists ($w^2 < 300 l.u.^2$), D_{micro} can be found for each temperature and it can be found that in the case of MC simulation $D_{micro}(325K) = 70D_{micro}(294K)$ (not shown). If one extrapolate the value of D from the second part of the FCS diffusion law ($300 l.u.^2 < w^2 < 1200 l.u.^2$), then it is found that $D_{micro}(325K) = 160D_{micro}(294K)$. This confirm that the shape of second part of the FCS diffusion law does contain more than only free diffusion. This cannot be verified for experimental laws since the first part of the FCS law is not accessible.

As defined above, τ_{d_0} is the value of τ_d for $w^2 = 0$. From Eq 12 it is found that :

$$\tau_{d_0} = K\tau_d^f(1 - 70S_g^n) \tag{13}$$

With increasing temperatures, the relative normalized gel area ($0 < S_g^n < 1$) is decreasing down to zero. In this study, S_g^n was determined from MC simulation of the DMPC/DSPC mixture at different temperatures. Fig. 2 shows evolution of τ_{d_0} with temperature for MC simulated FCS diffusion laws (Fig. 2A) and experimental FCS diffusion law (Fig. 2B) and the calculated values of τ_{d_0} as a function of S_g^n according to Eq. 13, adjusted to the lowest temperature value of τ_{d_0} by K constant. Both Fig. 2A and B shows a nice adequation of the calculated values with Eq. 13 and the numerical or experimental obtained values confirming the hypothesis that solid domains act as barriers to free-diffusion of the tracers. Although the present model is rather heuristic than accurate, it suggests that the gel confinement areas can be viewed as meshwork partially permeable barriers for the diffusion of fluorescent reporters, but not as impermeable domains, or as raft-like domains.

4 Size of domains and fluorescent dyes

C5 Bodipy PC has been shown to partition preferentially in liquid disordered phases (fluid phases) (11, 12) than in liquid ordered phase, raising therefore a question regarding the possibility for this fluorophore to explore equivalently solid and fluid phase in this study, this, even though such a partition haven't been, to our knowledge, published in the case of solid phase. It even have been suggested that C5 Bodipy PC could accumulate at the interface

between gel and liquid phases, leading therefore to uncorrect measurements. It is clear that if this is the case, one could argue that this could be the reason why two different scales in the domain size are seen in this work and that the one found experimentally is non relevant. In order to verify this hypothesis, FCS diffusion laws have been performed using an Atto647 head labeled Phosphatidyl Ethanolamine (13) as the fluorescent dye at temperatures around the first transition $gg : gf$ which is the main transition in the DMPC:DSPC 8:2 mol:mol system. Fig. 3 clearly shows that the same range of domain size is seen by both fluorescent dyes used in this study, discarding therefore the hypothesis that domain size obtained by experimental FCS diffusion laws are due to location of the dye where mismatches take place or that the differences seen between MC simulation and experimental FCS diffusion laws are due to a difference in the partitioning of fluorescent tracers.

5 Fit of the FCS diffusion laws assuming anomalous diffusion

As discussed in the main manuscript, anomalous diffusion can be use to describe the molecular movements in complex media. In this latter case, the mean square displacement is proportional to a power law of time according the following equation :

$$< r^2 >= \Gamma t^{\alpha} \tag{14}$$

with α the anomalous exponent and Γ an equivalent of diffusion coefficient in $m^2.s^{-\alpha}$. The Brownian diffusion is, in this more general context, a particular case where $\alpha = 1$. FCS diffusion laws obtained both experimentally and numerically in the DMPC:DSPC 8:2 mol:mol lipid mixture were fitted at different temperatures using the following equation :

$$\tau_d = \{\frac{w^2}{\Gamma}\}^{1/\alpha} \tag{15}$$

The values obtained for α are displayed as a function of temperature in Fig. 4. It clearly shows that α goes through a minimum at temperatures close to both transition $gg : gf$ and $gf : ff$. These temperatures are the one where the domain size are the highest as seen by FCS diffusion laws w_0^2 parameter. This correlation confirm that the system can be described using anomalous diffusion, but that, contrarily to linear fit of FCS diffusion laws, anomalous diffusion fit does not give any quantitative information on the size of the domains.

References

1. Vaz, W., E. Melo, and T. Thompson, 1989. Translational diffusion and fluid domain connectivity in a 2-component 2-phase phospholipid bilayer. *Biophys. J.* 56:869–876.

2. Wawrezinieck, L., H. Rigneault, D. Marguet, and P. Lenne, 2005. Fluorescence correlation spectroscopy diffusion laws to probe the submicron cell membrane organization. *Biophys. J.* 89:4029–4042.

3. Wenger, J., F. Conchonaud, J. Dintinger, L. Wawrezinieck, T. Ebbesen, H. Rigneault, D. Marguet, and P.-F. Lenne, 2007. Diffusion analysis within single nanometric apertures reveals the ultrafine cell membrane organization. *Biophys. J.* 92:913–919.

4. Sugar, I., T. Thompson, and R. Biltonen, 1999. Monte Carlo simulation of two-component bilayers: DMPC/DSPC mixtures. *Biophys. J.* 76:2099–2110.

5. Hac, A., H. Seeger, M. Fidorra, and T. Heimburg, 2005. Diffusion in two-component lipid membranes - A fluorescence correlation spectroscopy and Monte Carlo simulation study. *Biophys. J.* 88:317–333.

6. Wohland, T., R. Rigler, and H. Vogel, 2001. The standard deviation in fluorescence correlation spectroscopy. *Biophys. J.* 80:2987–2999.

7. Schatzel, K., 1985. New concepts in correlator design. *In* Institute of Physics Conference Series, Hilger, London, 175–184.

8. Petersen, N., P. Hoddelius, P. Wiseman, O. Seger, and K. Magnusson, 1993. Quantitation of membrane-receptor distribution by image correlation spectroscopy - Concept and application. *Biophys. J.* 65:1135–1146.

9. Almeida, P., W. Vaz, and T. Thompson, 1992. Lateral diffusion and percolation in 2-phase, 2-component lipid bilayers - Topology of the solid-phase domains inplane and across the lipid bilayer. *Biochemistry* 31:7198–7210.

10. Wiener, M., R. Suter, and J. Nagle, 1989. Structure of the fully hydrated gel phase of dipalmitoylphosphatidylcholine. *Biophys. J.* 55:315–325.

11. Wang, T., and J. Silvius, 2000. Different sphingolipids show differential partitioning into sphingolipid/cholesterol-rich domains in lipid bilayers. *Biophys. J.* 79:1478–1489.

12. Baumgart, T., G. Hunt, E. Farkas, W. Webb, and G. Feigenson, 2007. Fluorescence probe partitioning between Lo/Ld phases in lipid membranes. *BBA - Biomembranes* 1768:2182–2194.

13. Eggeling, C., C. Ringemann, R. Medda, G. Schwarzmann, K. Sandhoff, S. Polyakova, V. N. Belov, B. Hein, C. von Middendorff, A. Schoenle, and S. W. Hell, 2009. Direct observation of the nanoscale dynamics of membrane lipids in a living cell. *Nature* 457:1159–1162.

Table 1: **Monte-Carlo simulation parameters.** Parameters of the Monte Carlo simulation of DMPC-DSPC mixture. The indices g and f correspond to gel and fluid state respectively. Values are the one given in (5)

$T_{m,A} = 297.1K$	$\omega_{AA}^{gf} = 1353J.mol^{-1}$
$T_{m,B} = 327.9K$	$\omega_{BB}^{gf} = 1474J.mol^{-1}$
$\Delta H_A = 13.165kJ.mol^{-1}$	$\omega_{AB}^{gg} = 607J.mol^{-1}$
$\Delta H_B = 25.37kJ.mol^{-1}$	$\omega_{AB}^{ff} = 251J.mol^{-1}$
$\Delta S_A = 44.31J.mol^{-1}.K^{-1}$	$\omega_{AB}^{gf} = 1548J.mol^{-1}$
$\Delta S_B = 77.36J.mol^{-1}.K^{-1}$	$\omega_{AB}^{fg} = 1716J.mol^{-1}$

Table 2: **List and definition of variables used in the manuscript**

symbol	signification
g	Gel phase (equivalent to s solid phase).
f	Fluid phase (equivalent to l_d liquid disordered phase).
$g^{(2)}(\tau)$	Temporal autocorrelation function of the intensity fluctuation.
w	Waist of the laser.
τ_d	Diffusion time.
$f_{c,g}$	Fraction of lipids chains in gel state.
$r(f_{c,g})$	Probability of entering a diffusion step as a function of the environment.
r_0	Value of $r(f_{c,g})$ in a fully liquid environment ($f_{c,g} = 0$).
ΔE	Energy barrier to overcome in order to diffuse in a pure gel environment.
r_{state}	Probability for a lipid chain of becoming fluid when gel or inversely.
D_{forg}	Number of lipids of species A or B in gel (g) or fluid (f) state.
E_{AB}^{gf}	Internal energy of lipids of species A or B in gel (g) or fluid (f) state.
n_{AB}^{gf}	number of lipids of species A or B in gel (g) or fluid (f) state.
G	Gibbs energy of a lipid monolayer in a given configuration.
G_0	Gibbs energy of an all gel lipid matrix.
$\Delta H_{A,B}$	Calorimetric enthalpy of lipid specie A or B.
$\Delta S_{A,B}$	Melting entropies of pure lipid specie A or B.
$T_{m,A}, T_{m,B}$	Melting temperature of pure lipid specie A or B.
$\omega_{ij}^{\alpha\beta}$	Nearest-neighbor interaction parameters of a lipid chain specie i in state α with a lipid chain specie j in state β.
$I(r)$	Intensity of emitted fluorescence as a function of radial distance in MC simulation.
$g(\xi)$	spatial 1-D autocorrelation function of the intensity fluctuation.
A_{dom}	area occupied by a domain.
S_g	surface occupied by lipids in gel state.
S_f	surface occupied by lipids in fluid state.
S_g^n	fractional area of gel lipid ($0 < S_g^n < 1$).
$\langle a \rangle$	mean size occupied by a lipid (for simulation scaling purpose).
f_g	fraction of lipids in the gel state.
f_f	fraction of lipids in the fluid state.
a_g	area occupied by one lipid in the gel state.
a_f	area occupied by one lipid in the fluid state.
D_{micro}	Diffusion coefficient within a mesh of partially permeable barriers meshwork model.
S_{conf}	Confinement parameter in the mesh of partially permeable barriers meshwork model.
τ_d^{domain}	Diffusion time within a mesh of partially permeable barriers meshwork model.
τ_{conf}	Confinement time within a mesh of partially permeable barriers meshwork model.
τ_d^f	Diffusion time in fluid state.
τ_d^g	Diffusion time in gel state.
$D_{micro}(T)$	Pure Brownian diffusion coefficient as a function of temperature.
K, B	Dimensionless constants.
w_0^2	Value of the probed area w^2 for which $\tau_d = 0$.
$l.u.$	Lattice unit : $1(l.u)^2 = 1$ lipid.
D_{micro}^{gf}	Pure Brownian diffusion coefficient in gel or fluid lipids.
τ_{d_0}	Linear asymptotic extrapolation of the diffusion time (τ_d at $w^2 = 0$).
Γ	Anomalous diffusion coefficient.
α	Anomalous exponent of the diffusion process ($0 < \alpha < 2$).

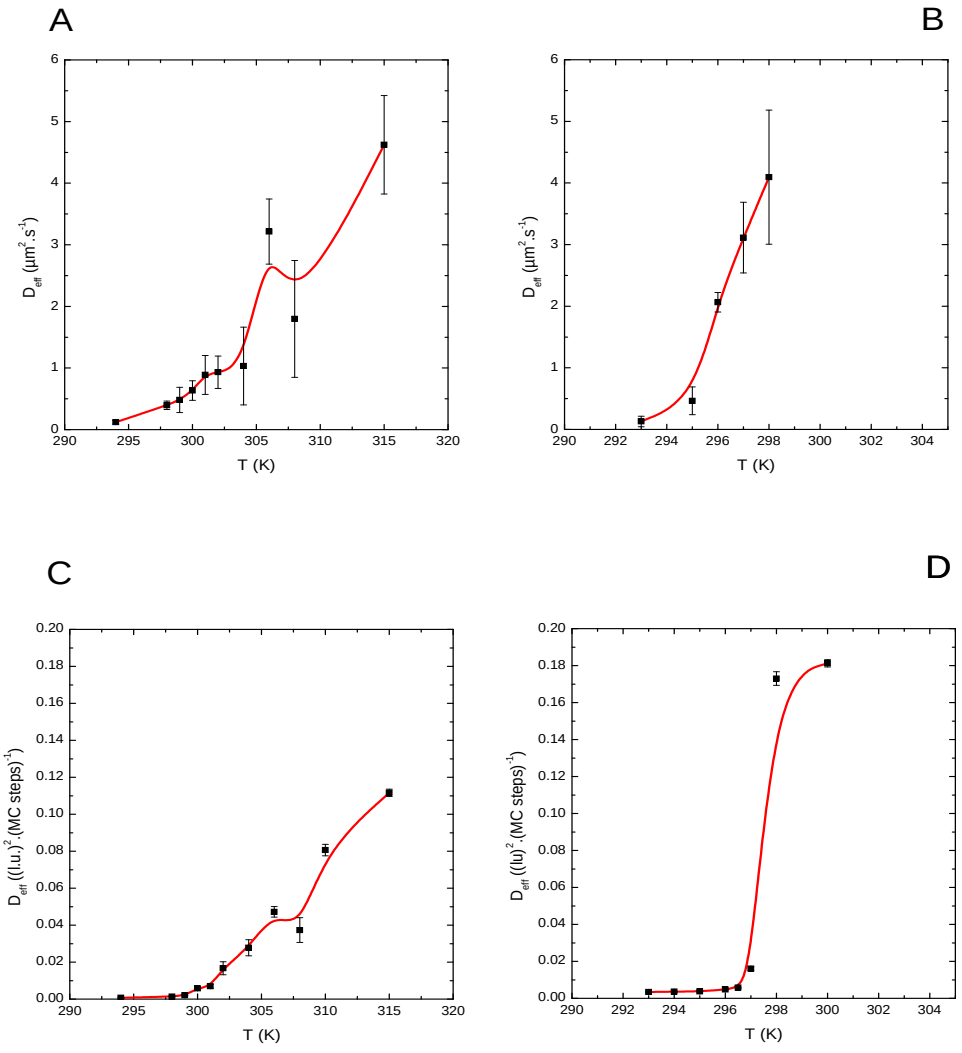

Figure 1: **Effective diffusion coefficient obtained by FCS diffusion laws.** Variation of the diffusion coefficient (D_{eff}) obtained by measuring the slope of the different fits using eq.5 of the main text of the FCS diffusion laws as a function of temperature. This clearly show, as expected, an increase in D_{eff} with temperature from a lower plateau (gel phase) to a higher one (liquid phase). Part A and B are values experimentally obtained whereas part C and D are numerically obtained for DMPC:DSPC 8:2 mol:mol and pure DMPC respectively.
Experimental point are linked by a solid curve polynomial fit to guide the eye.

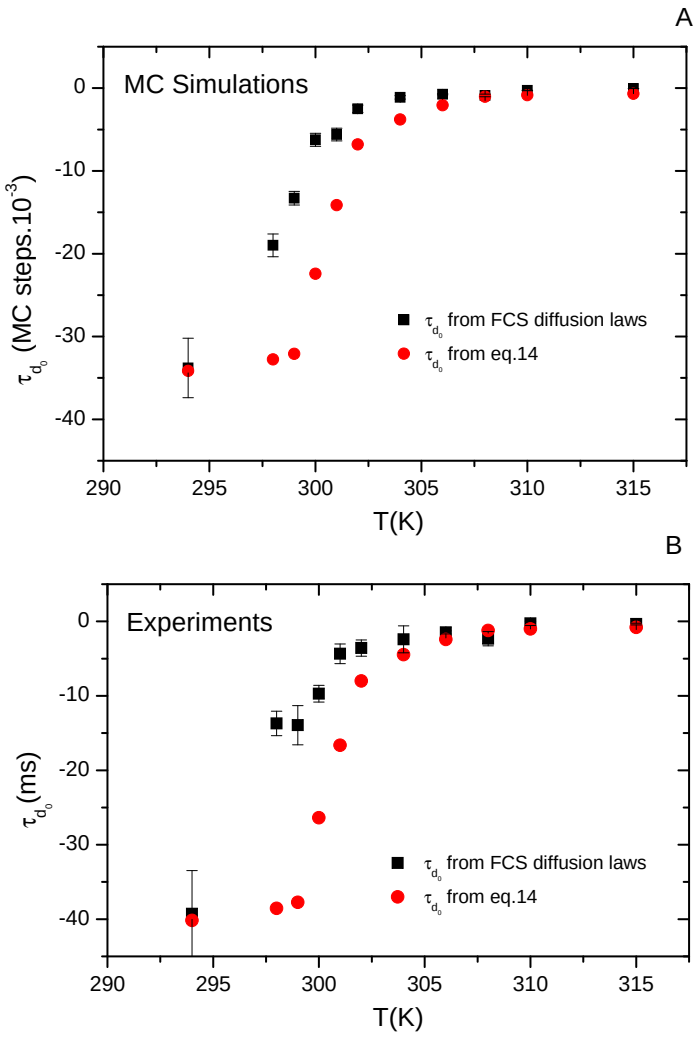

Figure 2: **Comparison of experimental and MC simulated τ_{d_0} to τ_{d_0} obtained from Eq. 13**
Part A. Comparison of τ_{d_0} obtained by linear fit of the asymptotic part of the simulated FCS diffusion laws to τ_{d_0} obtained by eq. 13 as a function of temperature (i.e. a function of normalized gel area).
Part B. Comparison of τ_{d_0} obtained by linear fit of the asymptotic part of the experimental FCS diffusion laws to τ_{d_0} obtained by eq. 13 as a function of temperature.
Both are normalized by means of K factor at 294K.

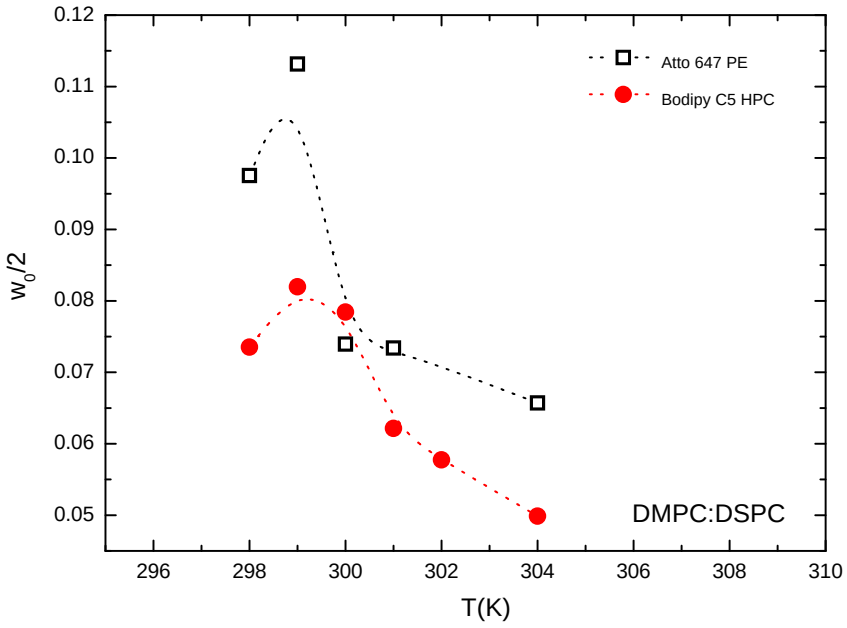

Figure 3: **Comparison of the mean radius of domains seen by different fluorescent dyes**
Bodipy C5 PC and Atto647 PE have been used to achieve FCS diffusion laws in DMPC:DSPC in order to determinate the mean radius of domains in the DMPC:DSPC 8:2 mol:mol lipid mixture. The figure shows that the same range of size of domains are seen by both dyes discarding any misleading effect on the determinated domain sizes due to the dye itself.

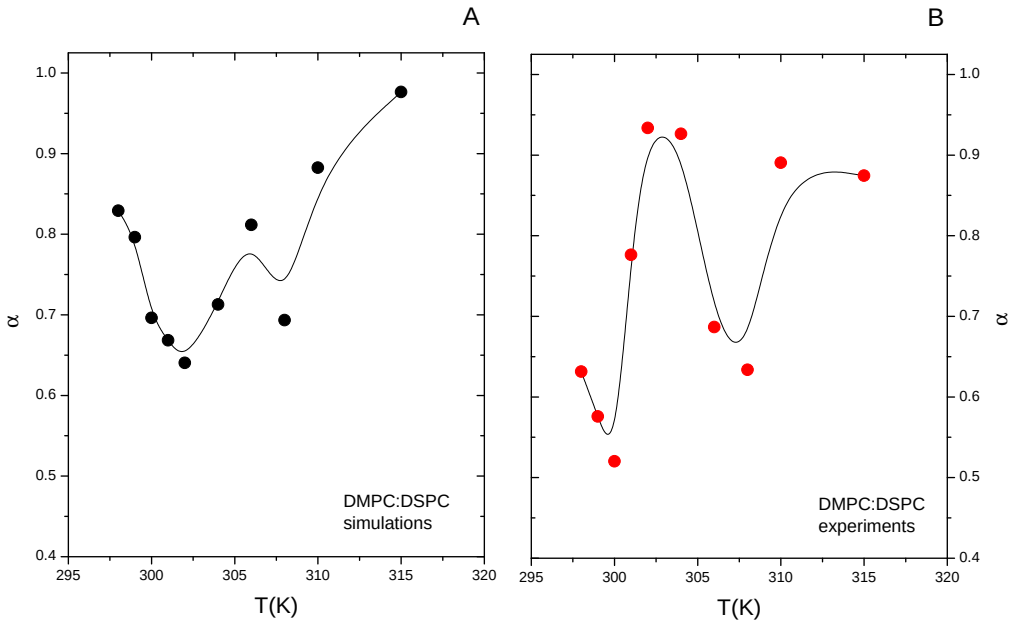

Figure 4: **Anomalous exponent α as a function of temperature**
Part A. Fit of the FCS diffusion laws obtained by MC numerical of the DMPC:DSPC 8:2 mol:mol mixture using eq. 15.
Part B. Fit of the FCS diffusion laws obtained experimentally on the DMPC:DSPC 8:2 mol:mol mixture using eq. 15.
In both cases, the value of the anomalous coefficient α is plotted vs. temperature *Experimental point are linked by a solid curve polynomial fit to guide the eye.*

Movie 1. Movie of tracers in MC simulation of DMPC:DSPC mixture

This movie is a stack of images obtained step by step by MC simulations. The total duration of the movie is 300 MC steps. Solid domains are represented in black, fluid domains in gray, the tracers being in white. Temperature is 302K.